

High-Resolution Magnetic Resonance Imaging of Cervicocranial Artery Dissection Imaging Features Associated With Stroke

Ye Wu, MD*; Fang Wu, MD*; Yuehong Liu, MD; Zhaoyang Fan, PhD; Marc Fisher, MD; Debiao Li, PhD; Weihai Xu, MD; Tao Jiang, MD; Jingliang Cheng, MD; Bin Sun, MD; Xunming Ji, MD, PhD; Qi Yang, MD, PhD

Background and Purpose—We aimed to systematically investigate the characteristics of cervicocranial artery dissection (CCAD) on high-resolution magnetic resonance imaging that are associated with acute ischemic stroke.

Methods—Patients with CCAD were recruited and divided into stroke and nonstroke groups. The lesion location, the presence of a double lumen, intimal flap, intramural hematoma, pseudoaneurysm, irregular surface, intraluminal thrombus, and other quantitative parameters of each dissected segment were reviewed. Multiple logistic regression was used to examine the association between imaging features of CCAD and ischemic stroke.

Results—A total of 145 affected vessels from 118 patients with CCAD were analyzed. Anterior circulation, intramural hematoma, irregular surface, intraluminal thrombus, and severe stenosis (>70%) on high-resolution magnetic resonance imaging were more prevalent in CCAD patient with stroke (54.4% versus 36.4%; $P=0.030$, 96.2% versus 84.8%; $P=0.017$, 74.7% versus 37.9%; $P<0.001$, 44.3% versus 4.5%; $P<0.001$, and 54.4% versus 31.8%; $P=0.008$, respectively). In multivariable logistic regression analysis, the presence of irregular surface and intraluminal thrombus on imaging were independently associated with acute ischemic stroke in CCAD with odds ratios of 4.29 (95% CI, 1.61–11.46, $P=0.004$) and 7.48 (95% CI, 1.64–34.07, $P=0.009$).

Conclusions—The current findings supported that the presence of irregular surface and intraluminal thrombus were related to stroke occurrence in patients with CCAD. High-resolution magnetic resonance imaging might give insights into pathogenesis of ischemic stroke in CCAD. It may be useful for individual prediction of ischemic stroke early in CCAD. (*Stroke*. 2019;50:00-00. DOI: 10.1161/STROKEAHA.119.026362.)

Key Words: angiography ■ artery dissection ■ embolism ■ magnetic resonance imaging ■ risk factor

Cervicocranial artery dissection (CCAD) is an important cause of ischemic stroke in young patients.¹ Population-based studies have reported that >50% of patients with CCAD presented with stroke or transient ischemic attack.^{2,3} Most strokes occur in the first few weeks after dissection.⁴ Early detection of high-risk imaging characteristics of CCAD may be useful to aid in the preventive treatment of patients with CCAD without stroke but at higher risk. Several studies have investigated the relationship between demographic characteristics, risk factors, and stroke in CCAD.⁵⁻⁷ The stroke subtypes of CCAD had been inferred to be embolization other than hemodynamic impairment, and artery-to-artery embolism is the major mechanism.⁸ Intimal damage and microthrombus formation may be

associated with artery-to-artery embolism. A recent study has investigated the radiological characteristics associated with ischemic stroke in patients suspected of CCAD using fat-suppressed T1-weighted imaging and T1-weighted flow-suppressed magnetization-prepared rapid acquisition gradient-recalled echo sequences.⁹ They showed that intramural hematoma detection significantly contributed to stroke in patients with suspected CCAD. We hypothesized that there would be identifiable imaging features that would be associated with stroke.

Multiple modalities (computed tomography, magnetic resonance imaging [MRI], and carotid artery ultrasound) have been used to complement each other to facilitate the diagnosis of CCAD.^{10,11} Nevertheless, definite diagnosis is often difficult

Received May 17, 2019; final revision received July 29, 2019; accepted August 9, 2019.

From the Departments of Radiology (Y.W., F.W., Y.L., Q.Y.) and Neurosurgery (X.J.), Xuanwu Hospital, Capital Medical University, Beijing, China; Biomedical Imaging Research Institute, Cedars Sinai Medical Center, Los Angeles, CA (Z.F., D.L.); Department of Neurology, Beth Israel Deaconess Medical Center, Boston, MA (M.F.); Department of Neurology, Peking Union Medical College Hospital, Chinese Academy of Medical Sciences, Beijing, China (W.X.); Department of Radiology, Chaoyang Hospital, Capital Medical University, Beijing, China (T.J.); Department of Radiology, The First Affiliated Hospital of Zhengzhou University, China (J.C.); and Department of Radiology, Fujian Medical University Union Hospital, Fuzhou, China (B.S.).

*Drs Y. Wu and F. Wu contributed equally.

Guest Editor for this article was Gregory W. Albers, MD.

The online-only Data Supplement is available with this article at <https://www.ahajournals.org/doi/suppl/10.1161/STROKEAHA.119.026362>.

Correspondence to Qi Yang, MD, PhD, Department of Radiology, Xuanwu Hospital, Capital Medical University, No. 45 Changchun St, Xicheng District, Beijing, China, 100053. Email: yangyangqiqi@gmail.com

© 2019 American Heart Association, Inc.

Stroke is available at <https://www.ahajournals.org/journal/str>

DOI: 10.1161/STROKEAHA.119.026362

because of the low sensitivity of these radiological methods for various signs, such as intramural hematoma, intimal flap, or double lumen.¹¹ Recently, high-resolution MRI (HRMRI) has been used in the evaluation of patients with CCAD.^{12–15} HRMRI provides direct visualization both of vessel wall abnormalities and an intraluminal thrombus.¹⁶ The potential contribution of individual risk factors and dissection imaging findings on HRMRI to stroke has not been well evaluated. Thus, the aim of this study was to investigate the imaging features that are associated with ischemic stroke in patients with CCAD.

Methods

Data Availability

Anonymized data not published within this article will be shared by request from any qualified investigator.

Standard Protocol Approvals, Registrations, and Patient Consents

The study was approved by the local Ethics Committee. Written informed consent was obtained from all patients in this study.

Participants

Between September 2013 and September 2018, patients with recent CCAD diagnosed by imaging techniques in our neurology department were recruited. All patients had neurological symptoms such as dizziness, headache, vomiting, sensory or motor disorders, transient ischemic attack, or ischemic stroke. The indication for doing HRMRI was suspected of dissection by carotid artery ultrasound or carotid computed tomography angiography. Head-neck combined HRMRI was performed within 28 days after symptom onset. Diffusion-weighted imaging (DWI) was performed within 7 days. Patients with DWI lesions but without clinical symptoms have been excluded. A diagnosis of CCAD was made if any pathognomonic signs of dissection (double lumen, intimal flap, intramural hematoma, and pseudoaneurysm) were identified on imaging methods, such as computed tomography angiography, magnetic resonance angiography, carotid artery ultrasound, digital subtraction angiography, and HRMRI. Ischemic stroke status was determined by focal onset of neurological symptoms and positive DWI. The following types of patients were excluded: (1) dissection accompanied by other cerebral vasculopathies (eg, Moyamoya disease, vasculitis, fibromuscular dysplasia, intracranial or carotid arteriosclerosis with $\geq 50\%$ stenosis, identifiable plaque component of a large lipid-rich necrotic core, or intraplaque hemorrhage¹⁷); (2) evidence of cardioembolism; (3) previous strokes or transient ischemic attacks; (4) history of transluminal intervention; and (5) patients with renal dysfunction (estimated glomerular filtration rate assessed by creatinine clearance < 60 mL/[min \cdot 1.73 m²]). The clinical characteristics including sex, age, history of trauma, recent infection, smoking, alcohol use, migraine, hypertension, hyperlipidemia, multiple lesions, and the time interval between symptom onset to HRMRI were recorded of each patient.

MRI Protocol

All patients underwent HRMRI using a 3-T MRI scanner (Magnetom Verio, Skyra, Prisma, Siemens, Erlangen, Germany) with a 32-channel integrated head/neck coil. HRMRI was acquired by using a pre-contrast and postcontrast 3-dimensional turbo spin-echo technique known as T1w-Sampling Perfection With Application-Optimized Contrast Using Different Flip Angle Evolutions.^{18,19} The parameters were as follows: repetition time=900 ms; echo time=14 ms; field of view=230 mm; matrix=288 \times 384; slices number=224; slice thickness=0.6 mm; voxel size=0.6 \times 0.6 \times 0.6 mm³; acquisition time=7 minutes. Postcontrast HRMRI was performed 5 minutes after the injection of single-dose (0.1 mmol per kg of bodyweight) gadolinium-based contrast agent (Magnevist; Schering, Berlin, Germany).

Image Interpretation

All DWI images were evaluated by the consensus of 2 neuroradiologists for the determination of a recent infarction.²⁰ The carotid artery (internal carotid artery), vertebral artery and basilar artery middle cerebral artery, posterior cerebral artery were included in the analysis. Dissected arteries were considered to be the cause of the stroke if the hyperintense lesions on DWI were detected in the vascular territory supplied by the branches distal to the site of the dissection. Dissected vessels without DWI abnormalities within the vascular territory were classified into nonstroke group, including patients with transient ischemic attack.

HRMRI images were interpreted separately by 2 experienced neuroradiologists who were blinded to the DWI and clinical information using commercial software (Osirix MD; Pixmeo SARL, Switzerland; and Vessel Analysis; Surway Star Technology, China). All Source images and curved multiplanar reformation images were used for assessment. The sites of dissected vessels (intracranial or extracranial, anterior or posterior, single, or multiple) on HRMRI were recorded. The presence of a double lumen, intimal flap, intramural hematoma, pseudoaneurysm, irregular surface, intraluminal thrombus, and other quantitative parameters of each dissected segment was reviewed.²¹ The double lumen sign was defined as blood flow that was divided into a true and a false lumen.²² An intimal flap was considered as a curvilinear and isointense line crossing the flow void lumen or between a hyperintense hematoma that extended to the sidewall.^{15,23} Intramural hematoma was defined as crescent-shaped thickening of the arterial wall that was isointense/hyperintense on precontrast images.^{11,16,24} Pseudoaneurysm was defined as the diameter of aneurysmal vessels dilated over 1.5 \times than the normal distal artery.²⁵ Irregular surface was defined as a discontinuity of the juxtaluminal surface of the intramural hematoma. Intraluminal thrombus was defined as a hyperintense filling within the lumen on precontrast images, as well as an area of intraluminal contrast enhancement on postcontrast images.^{16,26} (Figure 1). The lesion length was measured on curved planar reformation images of HRMRI. The stenosis degree at the most stenotic site was defined as (1-lesion lumen diameter/reference lumen diameter) $\times 100\%$. The stenosis degree was graded as $\leq 49\%$, 50%–69%, and $\geq 70\%$, according to the NASCET (North American Symptomatic Carotid Endarterectomy Trial) method of measurement.²⁷ The characteristics of signal intensity of intramural hematoma (homogeneous or heterogeneous) and contrast enhancement ratio of intramural hematoma (signal intensity–postcontrast/signal intensity–precontrast 100%) were measured. Any discrepancies between the reviewers were resolved by consensus. After an interval of 2 months, 1 reader reassessed all HRMRI studies.

Statistical Analysis

All continuous data were described as the mean value \pm SDs, and categorical data were expressed as frequencies (percentage). Categorical variables were analyzed using a χ^2 test, and continuous variables were compared using a *t* test or Mann-Whitney *U* test between the 2 groups. Variables were entered into multivariate analysis model if they were $P \leq 0.1$ on the univariate analysis. Multivariate logistic regression analysis with the method of enter stepwise was conducted to determine independent predictors of the stroke. A value of $P < 0.05$ was considered to indicate statistical significance. The intraobserver and interobserver agreement in qualitative CCAD characteristics were evaluated by using Cohen κ coefficient, whereas quantitative CCAD characteristics measurement were evaluated by intraclass correlation coefficient. Multiple collinearity of variables were diagnosed by tolerance < 0.1 or variance inflation factor > 10 . All statistical analysis was performed with SPSS 20.0 (IBM).

Results

Clinical Characteristics

A total of 118 patients with CCAD (80 men; mean age, 40.3 \pm 10.1 years) were recruited, including 71 patients with stroke and 47 patients without stroke but with neurological

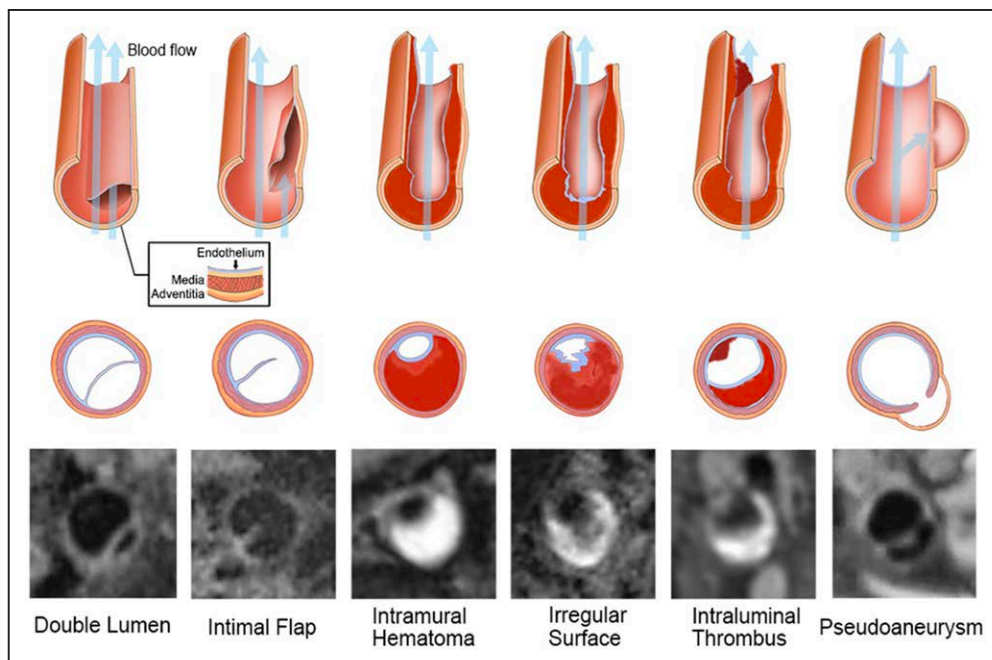


Figure 1. Diagram of the characteristics of cervicocranial artery dissection and corresponding typical high-resolution magnetic resonance imaging images.

symptoms. All clinical characteristics of patients were presented in Table 1.

Location of CCAD Lesions

A total of 145 dissecting arteries were included, with multiple vessels involved in 21 (17.8%) patients. Sixty-six (45.5%) of the 145 lesions were found in the internal carotid artery, 71 (49.0%) in the vertebral artery, 6 (4.1%) in the basilar artery, 1 (0.7%) in middle cerebral artery, and 1 (0.7%) in posterior cerebral artery. Seventy-nine (54.5%) affected vessels were classified as in the stroke group, and 66 (45.5%) were in the nonstroke group. The dissected arteries in stroke group were more likely to be located in the anterior circulation than that in nonstroke group (54.4% versus 36.4%; $P=0.030$).

Intraobserver and Interobserver Agreement on HRMRI Measurements

For the intrareader agreement in the identification of the presence of double lumen, intimal flap, intramural hematoma, pseudoaneurysm, irregular surface, intraluminal thrombus, and heterogeneous signal intensity of intramural hematoma, the K values were 0.91, 0.87, 0.86, 0.85, 0.96, 0.81, and 0.95, respectively. The interobserver reproducibility for the presence of double lumen, intimal flap, intramural hematoma, pseudoaneurysm, irregular surface, intraluminal thrombus, and heterogeneous signal intensity of intramural hematoma had K values of 0.91, 0.89, 0.90, 0.81, 0.79, 0.95, and 0.91, respectively. The intraclass correlation coefficient of length and contrast enhancement ratio of intramural hematoma was 0.93 and 0.84, with all $P<0.05$, respectively.

HRMRI Characteristics of CCAD

An intramural hematoma, irregular surface and intraluminal thrombus on HRMRI were more frequent in the stroke group,

compared with the nonstroke group (96.2% versus 84.8%; $P=0.017$, 74.7% versus 37.9%; $P<0.001$, and 44.3% versus 4.5%; $P<0.001$, respectively). Severe stenosis (stenosis degree $>70%$) was more frequent in the stroke group than in the non-stroke group (54.4% versus 31.8%; $P=0.008$). However, other HRMRI features, including the presence of a double lumen, an intimal flap, the length of dissecting artery, heterogeneous signal intensity, and enhancement of intramural hematoma were not significantly different between the 2 groups (All $P > 0.05$). Details of the HRMRI features of the 2 groups were described in Table 2.

Table 1. Clinical Characteristics of 145 Dissecting Arteries

| | Stroke Group; n=79 | Nonstroke Group; n=66 | P Value |
|---|--------------------|-----------------------|---------|
| Age, y, mean (SD) | 40.4±9.7 | 40.3±10.6 | 0.936 |
| Male patients, N (%) | 64 (81.0) | 31 (47.0) | < 0.001 |
| BMI, kg/m ² , mean(SD) | 24.1±3.3 | 24.1±3.2 | 0.970 |
| Risk factors, N (%) | | | |
| History of trauma | 26 (32.9) | 28 (42.4) | 0.238 |
| Recent infection | 11 (13.9) | 10 (15.2) | 0.834 |
| Smoking | 33 (41.8) | 23 (34.8) | 0.394 |
| Alcohol use | 35 (43.8) | 23 (34.8) | 0.274 |
| Migraine | 11 (13.9) | 8 (12.1) | 0.749 |
| Hypertension | 17 (21.5) | 13 (19.7) | 0.787 |
| Hyperlipidemia | 27 (34.2) | 22 (33.3) | 0.915 |
| NIHSS, median (interquartile range) | 3 (1,8) | 0 (0,0) | 0.000 |
| Onset to HRMRI time, median (interquartile range) | 11 (6–20) | 14 (11–20) | 0.079 |

BMI indicates body mass index; HRMRI, high-resolution magnetic resonance imaging; and NIHSS, National Institutes of Health Stroke Scale.

Table 2. HRMRI Features of the 2 Groups

| | Total N=145 | Stroke Group; n=79 | Nonstroke Group; n=66 | P Value |
|--|----------------|--------------------------|-----------------------------|---------|
| Anterior circulation, N (%) | 67 (46.2) | 43 (54.4) | 24 (36.4) | 0.030 |
| Extracranial, N (%) | 117 (80.7) | 65 (82.3) | 52 (78.8) | 0.596 |
| Double lumen, N (%) | 25 (17.2) | 10 (12.7) | 15 (22.7) | 0.110 |
| Intimal flap, N (%) | 49 (33.8) | 24 (30.4) | 25 (37.9) | 0.342 |
| Intramural hematoma, N (%) | 132 (91.0) | 76 (96.2) | 56 (84.8) | 0.017 |
| Pseudoaneurysm, N (%) | 27 (18.6) | 9 (11.4) | 18 (27.3) | 0.014 |
| Irregular surface, N (%) | 84 (57.9) | 59 (74.7) | 25 (37.9) | < 0.001 |
| Intraluminal thrombus, N (%) | 38 (26.2) | 35 (44.3) | 3 (4.5) | < 0.001 |
| Length, cm, mean (SD) | 4.4 (2.8) | 4.5 (2.6) | 4.3 (3.1) | 0.767 |
| Stenosis degree | | | | |
| ≤49% | 52 (35.9) | 20 (25.3) | 32 (48.5) | 0.008 |
| 50%–69% | 29 (20.0) | 16 (20.3) | 13 (19.7) | |
| 70%–100% | 64 (44.1) | 43 (54.4) | 21 (31.8) | |
| Heterogeneous signal of intramural hematoma, N (%) | 85 (57.0) | 50 (63.3) | 35 (53.0) | 0.212 |
| Enhancement of intramural hematoma, %, mean (SD) | 120 (35) | 118 (29) | 122 (43) | 0.603 |

HRMRI indicates high-resolution magnetic resonance imaging.

Association of HRMRI Features With Stroke

Intramural hematoma, non-pseudoaneurysm, irregular surface, intraluminal thrombus, degree of stenosis, as well as anterior circulation location showed significant associations

with ischemic stroke in the univariate analysis ($P<0.05$), then all variables with $P<0.1$ were used as input variables for the multivariate logistic regression analysis. Irregular surface and intraluminal thrombus remained significant in the multivariate analysis ($P<0.05$), with odds ratios of 4.29 (95% CI, 1.61–11.46) and 7.48 (95% CI, 1.64–34.07; Table 3 and Figures 2 and 3). There was no interaction between intramural hematoma, pseudoaneurysm, irregular surface, intraluminal thrombus, and degree of stenosis in regression analysis with the tolerance was all >0.1 and variance inflation factor <10 . Collinear diagnostic features were shown in Table I in the [online-only Data Supplement](#).

Discussion

In this study, we found a higher prevalence of intramural hematoma, irregular surface, intraluminal thrombus, and severe stenosis in patients with CCAD with stroke. Multivariate analysis showed that the presence of irregular surface and intraluminal thrombus were independently associated with the occurrence of acute ischemic stroke. Therefore, it is understandable that these high-risk imaging features may help to better understand the relationship between unstable CCAD, formation of blood clots, and embolic stroke.

CCAD implies a tear in the wall of the artery leading to the intrusion of blood within the layers of an arterial wall. An important pathological feature of symptomatic CCAD is that the affected vessel wall becomes the nidus for distal embolization. Previous studies demonstrated that intraluminal contrast enhancement on HRMRI, representing intraluminal thrombus formation, is strongly correlated with ischemic symptoms in patients with spontaneous CCAD.²⁶ In our study, a hyperintense signal was more likely to be found on the dissected vessel

Table 3. HRMRI Features of the 2 Groups

| | Univariate Logistic Regression | | | Multivariate Logistic Regression | | |
|---|--------------------------------|--------------|---------|----------------------------------|--------------|---------|
| | OR | 95% CI | P Value | OR | 95% CI | P Value |
| Anterior circulation | 2.090 | 1.071–4.081 | 0.031* | 1.837 | 0.788–4.284 | 0.159 |
| Extracranial | 1.250 | 0.547–2.854 | 0.596 | | | |
| Double lumen | 0.493 | 0.205–1.186 | 0.114 | | | |
| Intimal flap | 0.716 | 0.359–1.428 | 0.342 | | | |
| Intramural hematoma | 3.348 | 0.998–11.229 | 0.050* | 4.045 | 0.790–20.725 | 0.094 |
| Pseudoaneurysm | 0.343 | 0.142–0.827 | 0.017* | 0.485 | 0.136–1.736 | 0.266 |
| Irregular surface | 4.838 | 2.378–9.843 | <0.001* | 4.289 | 1.605–11.462 | 0.004 |
| Intraluminal thrombus | 16.705 | 4.832–57.746 | <0.001* | 7.476 | 1.640–34.074 | 0.009 |
| Length | 1.018 | 0.906–1.144 | 0.765 | | | |
| Stenosis degree | | | 0.010* | | | 0.572 |
| 50%–69% | 1.969 | 0.784–4.945 | 0.149 | 1.251 | 0.403–3.881 | 0.698 |
| 70%–100% | 3.276 | 1.525–7.037 | 0.002 | 0.687 | 0.227–2.077 | 0.506 |
| Heterogeneous signal of intramural hematoma | 1.527 | 0.785–2.971 | 0.212 | | | |
| Enhancement of intramural hematoma | 0.654 | 0.220–1.948 | 0.446 | | | |

HRMRI indicates high-resolution magnetic resonance imaging; and OR, odds ratio.

* $P<0.1$.

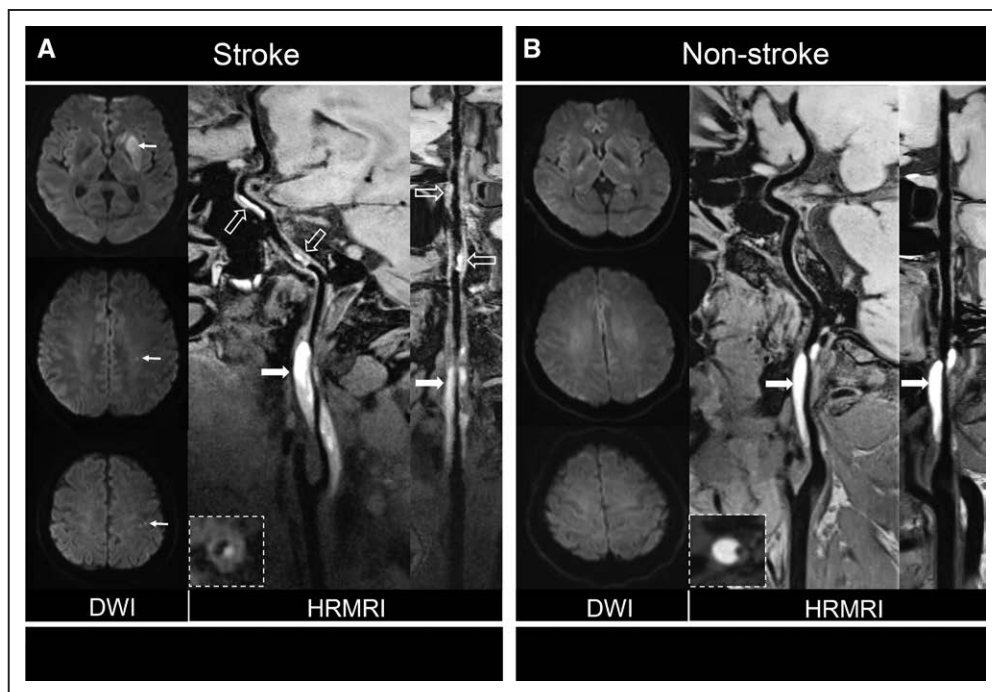


Figure 2. Comparison of patients with cervicocranial artery dissection with or without ischemic stroke. **A**, Diffusion-weighted imaging (DWI) showed acute ischemic stroke in left basal ganglia and centrum ovale (arrows) of 48 y of male patient. Curved planar reformation of high-resolution magnetic resonance imaging (HRMRI) demonstrated intramural hematoma (arrows) inner the vessel wall of C1 segment of left internal carotid artery (ICA) and distal intraluminal thrombus (dashed arrows) on the vessel wall of C2 and C4 segments of the ICA. Stretched curved planar reformation of HRMRI image depicted irregular surface and intraluminal thrombus. **B**, DWI showed no ischemic stroke in a 37-y-old female patient. Curved planar reformation of HRMRI image depicted a smooth vessel wall surface (arrows) without intraluminal thrombus. Stretched curved planar reformation of right ICA demonstrated the intramural hematoma and normal distal vessel wall.

wall of stroke patients (44.3% versus 4.5%, $P < 0.001$), which represents fresh intraluminal thrombus. The findings of intraluminal thrombus on HRMRI in our study supports previous research findings that thromboembolism is the most common stroke mechanism in patients with CCAD.⁸ Consistent with previous similar studies in carotid artery atherosclerosis, intraluminal thrombosis was a significant predictors of ischemic stroke (odds ratio, 7.48; 95% CI, 1.64–34.1, $P = 0.009$).²⁸

An irregular surface is another high-risk characteristic of CCAD associated with ischemic stroke observed in our study. Similarly, studies of carotid atherosclerotic plaques have revealed that an irregular surface is a risk factor for thrombosis formation and is associated with an increased risk of transient ischemic attack/stroke.^{29,30} The irregular surface of dissecting artery may represent intimal damage which may lead to microthrombus formation, consequently be correlated to ischemic stroke. In patients without stroke, we speculate this

may due to the uneven fluctuation caused by different stages of intramural hematoma without intimal damage.

A double lumen and intimal flap are important imaging features for CCAD diagnosis; however, in our study, they did not differ between the 2 groups. We found that patients with CCAD with stroke were more likely to have intramural hematoma, severe stenosis/occlusion. Intramural hematoma may represent a state in which blood flow tends to be coagulated or accumulated inside the false lumen. Severe stenosis/occlusion as can be associated with hypoperfusion and a greater risk of thrombogenesis resulting in ischemic stroke.³¹ However, our multivariate analysis demonstrated that the occurrence of stroke was not influenced by the degree of stenosis indicating that hemodynamic impairment may be a less important cause of stroke in patients with CCAD.³²

CCAD tends to affect multiple arterial segments and develop simultaneously in intracranial and extracranial

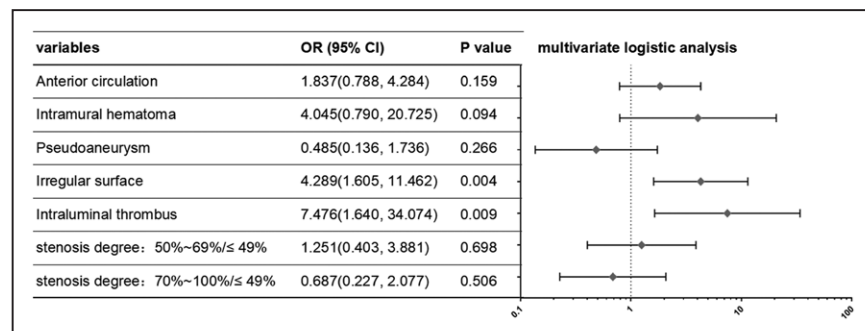


Figure 3. Odds ratio (OR) and 95% CI of stroke group vs nonstroke group on the basis of multivariate logistic regression for each feature.

vessels.^{33,34} In our study, we found intraluminal thrombus usually forms in the distal segments of the dissected vessel. Conventional HRMRI has limited coverage and does not allow the visualization of both extracranial and intracranial vessels.^{24,35,36} In the current study, we used 3-dimensional HRMRI technique with an integrated head-neck coil, which provided larger vessel coverage and higher spatial resolution, enabling a more comprehensive evaluation of the extracranial and intracranial vessels. The complementary information with HRMRI of vessel wall and vessel lumen may facilitate individualized risk stratification of CCAD. However, whether patients with these high-risk features could benefit from antithrombotic prophylaxis needs to be further investigated in future studies.

This study has several limitations. First, because this is a cross-sectional study, additional prospective studies are still needed to determine the predictive power of these imaging characteristics in occurrence of ischemic stroke. Second, the low rate of intracranial dissection indicates the potentially selective bias of our study. Large-scaled studies are needed to investigate the relationship between pseudoaneurysms and subarachnoid hemorrhage. Third, HRMRI studies were performed within 28 days after symptom onset in this study. Recent follow-up studies of CCAD have shown that the dissection may recover in short term.^{37,38} Thus, the dynamic nature of CCAD may affect the findings of high-risk features of dissected vessel wall. Finally, a separate validation cohort was absent due to the limited sample size in this single-center study.

In conclusion, irregular surface and an intraluminal thrombus were associated with stroke occurrence in patients with CCAD and may be useful for individual risk assessment early after clinical presentation.

Acknowledgments

We thank the patients involved in the study and appreciate the contribution of all investigators for our study.

Sources of Funding

This work was partially supported by National Science Foundation of China (No. 91749127 and No. 81830056), Beijing Natural Science Foundation (No. 7191003), Beijing Municipal Administration of Hospitals Clinical Medicine Development of Special Funding Support (ZYLX201706), and National Institutes of Health/National Heart, Lung, and Blood Institute 1 R01 HL147355.

Disclosures

None.

References

- Putaalaa J, Metso AJ, Metso TM, Konkola N, Kraemer Y, Haapaniemi E, et al. Analysis of 1008 consecutive patients aged 15 to 49 with first-ever ischemic stroke: the Helsinki young stroke registry. *Stroke*. 2009;40:1195–1203. doi: 10.1161/STROKEAHA.108.529883
- Touzé E, Gauvrit JY, Moulin T, Meder JF, Bracard S, Mas JL; Multicenter Survey on Natural History of Cervical Artery Dissection. Risk of stroke and recurrent dissection after a cervical artery dissection: a multicenter study. *Neurology*. 2003;61:1347–1351. doi: 10.1212/01.wnl.0000094325.95097.86
- Lee VH, Brown RD Jr, Mandrekar JN, Mokri B. Incidence and outcome of cervical artery dissection: a population-based study. *Neurology*. 2006;67:1809–1812. doi: 10.1212/01.wnl.0000244486.30455.71

- Morris NA, Merkler AE, Gialdini G, Kamel H. Timing of Incident Stroke Risk After Cervical Artery Dissection Presenting Without Ischemia. *Stroke*. 2017;48:551–555. doi: 10.1161/STROKEAHA.116.015185
- von Sarnowski B, Schminke U, Grittner U, Fazekas F, Tanislav C, Kaps M, et al. Cervical artery dissection in young adults in the stroke in young Fabry patients (sifap1) study. *Cerebrovasc Dis*. 2015;39:110–121. doi: 10.1159/000371338
- Arnold M, Kurmann R, Galimanis A, Sarikaya H, Stapf C, Gralla J, et al. Differences in demographic characteristics and risk factors in patients with spontaneous vertebral artery dissections with and without ischemic events. *Stroke*. 2010;41:802–804. doi: 10.1161/STROKEAHA.109.570655
- Debette S, Metso T, Pezzini A, Abboud S, Metso A, Leys D, et al; Cervical Artery Dissection and Ischemic Stroke Patients (CADISP) Group. Association of vascular risk factors with cervical artery dissection and ischemic stroke in young adults. *Circulation*. 2011;123:1537–1544. doi: 10.1161/CIRCULATIONAHA.110.000125
- Morel A, Naggara O, Touzé E, Raymond J, Mas JL, Meder JF, et al. Mechanism of ischemic infarct in spontaneous cervical artery dissection. *Stroke*. 2012;43:1354–1361. doi: 10.1161/STROKEAHA.111.643338
- McNally JS, Hinkley PJ, Sakata A, Eisenmenger LB, Kim SE, De Havenon AH, et al. Magnetic resonance imaging and clinical factors associated with ischemic stroke in patients suspected of cervical artery dissection. *Stroke*. 2018;49:2337–2344. doi: 10.1161/STROKEAHA.118.021868
- Debette S, Leys D. Cervical-artery dissections: predisposing factors, diagnosis, and outcome. *Lancet Neurol*. 2009;8:668–678. doi: 10.1016/S1474-4422(09)70084-5
- Rodallec MH, Marteau V, Gerber S, Desmottes L, Zins M. Craniocervical arterial dissection: spectrum of imaging findings and differential diagnosis. *Radiographics*. 2008;28:1711–1728. doi: 10.1148/rg.286085512
- Edjlali M, Roca P, Rabrait C, Naggara O, Oppenheim C. 3D fast spin-echo T1 black-blood imaging for the diagnosis of cervical artery dissection. *AJNR Am J Neuroradiol*. 2013;34:E103–E106. doi: 10.3174/ajnr.A3261
- Han M, Rim NJ, Lee JS, Kim SY, Choi JW. Feasibility of high-resolution MR imaging for the diagnosis of intracranial vertebral-basilar artery dissection. *Eur Radiol*. 2014;24:3017–3024. doi: 10.1007/s00330-014-3296-5
- Schwarz F, Strobl FF, Cyran CC, Helck AD, Hartmann M, Schindler A, et al. Reproducibility and differentiation of cervical arteriopathies using *in vivo* high-resolution black-blood MRI at 3 T. *Neuroradiology*. 2016;58:569–576. doi: 10.1007/s00234-016-1665-2
- Hunter MA, Santosh C, Teasdale E, Forbes KP. High-resolution double inversion recovery black-blood imaging of cervical artery dissection using 3T MR imaging. *AJNR Am J Neuroradiol*. 2012;33:E133–E137. doi: 10.3174/ajnr.A2599
- Bachmann R, Nassenstein I, Kooijman H, Dittrich R, Kugel H, Niederstadt T, et al. Spontaneous acute dissection of the internal carotid artery: high-resolution magnetic resonance imaging at 3.0 tesla with a dedicated surface coil. *Invest Radiol*. 2006;41:105–111.
- Saba L, Yuan C, Hatsukami TS, Balu N, Qiao Y, DeMarco JK, et al; Vessel Wall Imaging Study Group of the American Society of Neuroradiology. Carotid Artery Wall imaging: perspective and guidelines from the ASNR vessel wall imaging study group and expert consensus recommendations of the American society of neuroradiology. *AJNR Am J Neuroradiol*. 2018;39:E9–E31. doi: 10.3174/ajnr.A5488
- Fan Z, Yang Q, Deng Z, Li Y, Bi X, Song S, et al. Whole-brain intracranial vessel wall imaging at 3 Tesla using cerebrospinal fluid-attenuated T1-weighted 3D turbo spin echo. *Magn Reson Med*. 2017;77:1142–1150. doi: 10.1002/mrm.26201
- Yang Q, Deng Z, Bi X, Song SS, Schlick KH, Gonzalez NR, et al. Whole-brain vessel wall MRI: a parameter tune-up solution to improve the scan efficiency of three-dimensional variable flip-angle turbo spin-echo. *J Magn Reson Imaging*. 2017;46:751–757. doi: 10.1002/jmri.25611
- Sacco RL, Kasner SE, Broderick JP, Caplan LR, Connors JJ, Culebras A, et al; American Heart Association Stroke Council, Council on Cardiovascular Surgery and Anesthesia; Council on Cardiovascular Radiology and Intervention; Council on Cardiovascular and Stroke Nursing; Council on Epidemiology and Prevention; Council on Peripheral Vascular Disease; Council on Nutrition, Physical Activity and Metabolism. An updated definition of stroke for the 21st century: a statement for healthcare professionals from the American Heart Association/American Stroke Association. *Stroke*. 2013;44:2064–2089. doi: 10.1161/STR.0b013e318296aeca

21. Jung SC, Kim HS, Choi CG, Kim SJ, Lee DH, Suh DC, et al. Quantitative analysis using high-resolution 3T MRI in acute intracranial artery dissection. *J Neuroimaging*. 2016;26:612–617. doi: 10.1111/jon.12357
22. Drapkin AJ. The double lumen: a pathognomonic angiographic sign of arterial dissection? *Neuroradiology*. 2000;42:203–205.
23. Uemura M, Terajima K, Suzuki Y, Watanabe M, Akaiwa Y, Katada S, et al. Visualization of the intimal flap in intracranial arterial dissection using high-resolution 3T MRI. *J Neuroimaging*. 2017;27:29–32. doi: 10.1111/jon.12380
24. Takano K, Yamashita S, Takemoto K, Inoue T, Kuwabara Y, Yoshimitsu K. MRI of intracranial vertebral artery dissection: evaluation of intramural haematoma using a black blood, variable-flip-angle 3D turbo spin-echo sequence. *Neuroradiology*. 2013;55:845–851. doi: 10.1007/s00234-013-1183-4
25. Wang Y, Lou X, Li Y, Sui B, Sun S, Li C, et al. Imaging investigation of intracranial arterial dissecting aneurysms by using 3 T high-resolution MRI and DSA: from the interventional neuroradiologists' view. *Acta Neurochir (Wien)*. 2014;156:515–525. doi: 10.1007/s00701-013-1989-1
26. Coppenrath E, Lenz O, Sommer N, Lummel N, Linn J, Treitl K, et al. Clinical significance of intraluminal contrast enhancement in patients with spontaneous cervical artery dissection: a black-blood MRI study. *Rofo*. 2017;189:624–631. doi: 10.1055/s-0043-104632
27. Eliasziw M, Smith RF, Singh N, Holdsworth DW, Fox AJ, Barnett HJ. Further comments on the measurement of carotid stenosis from angiograms. North American Symptomatic Carotid Endarterectomy Trial (NASCET) Group. *Stroke*. 1994;25:2445–2449. doi: 10.1161/01.str.25.12.2445
28. McNally JS, McLaughlin MS, Hinckley PJ, Treiman SM, Stoddard GJ, Parker DL, et al. Intraluminal thrombus, intraplaque hemorrhage, plaque thickness, and current smoking optimally predict carotid stroke. *Stroke*. 2015;46:84–90. doi: 10.1161/STROKEAHA.114.006286
29. Wasserman BA, Smith WI, Trout HH III, Cannon RO III, Balaban RS, Arai AE. Carotid artery atherosclerosis: *in vivo* morphologic characterization with gadolinium-enhanced double-oblique MR imaging initial results. *Radiology*. 2002;223:566–573. doi: 10.1148/radiol.2232010659
30. Troyer A, Saloner D, Pan XM, Velez P, Rapp JH; Assessment of Carotid Stenosis by Comparison with Endarterectomy Plaque Trial Investigators. Major carotid plaque surface irregularities correlate with neurologic symptoms. *J Vasc Surg*. 2002;35:741–747.
31. Markus H, Cullinane M. Severely impaired cerebrovascular reactivity predicts stroke and TIA risk in patients with carotid artery stenosis and occlusion. *Brain*. 2001;124(pt 3):457–467. doi: 10.1093/brain/124.3.457
32. Naggara O, Morel A, Touzé E, Raymond J, Mas JL, Meder JF, et al. Stroke occurrence and patterns are not influenced by the degree of stenosis in cervical artery dissection. *Stroke*. 2012;43:1150–1152. doi: 10.1161/STROKEAHA.111.639021
33. Béjot Y, Aboa-Eboulé C, Debette S, Pezzini A, Tatlisumak T, Engelter S, et al; CADISP Group. Characteristics and outcomes of patients with multiple cervical artery dissection. *Stroke*. 2014;45:37–41. doi: 10.1161/STROKEAHA.113.001654
34. Thomas LC, Rivett DA, Parsons M, Levi C. Risk factors, radiological features, and infarct topography of craniocervical arterial dissection. *Int J Stroke*. 2014;9:1073–1082. doi: 10.1111/j.1747-4949.2012.00912.x
35. Cuvinciu V, Viallon M, Momjian-Mayor I, Sztajzel R, Pereira VM, Lovblad KO, et al. 3D fat-saturated T1 SPACE sequence for the diagnosis of cervical artery dissection. *Neuroradiology*. 2013;55:595–602. doi: 10.1007/s00234-013-1141-1
36. Natori T, Sasaki M, Miyoshi M, Ohba H, Oura MY, Narumi S, et al. Detection of vessel wall lesions in spontaneous symptomatic vertebrobasilar artery dissection using T1-weighted 3-dimensional imaging. *J Stroke Cerebrovasc Dis*. 2014;23:2419–2424. doi: 10.1016/j.jstrokecerebrovasdis.2014.05.019
37. Heldner MR, Nedelcheva M, Yan X, Slotboom J, Mathier E, Hulliger J, et al. Dynamic changes of intramural hematoma in patients with acute spontaneous internal carotid artery dissection. *Int J Stroke*. 2015;10:887–892. doi: 10.1111/ijs.12553
38. Habs M, Pfefferkorn T, Cyran CC, Grimm J, Rominger A, Hacker M, et al. Age determination of vessel wall hematoma in spontaneous cervical artery dissection: a multi-sequence 3T cardiovascular magnetic resonance study. *J Cardiovasc Magn Reson*. 2011;13:76. doi: 10.1186/1532-429X-13-76

Stroke